HOKKAIDO UNIVERSITY

Title	Adsorption behavior of bisphenol-A and diethyl phthalate onto bubble surface in nonfoaming adsorptive bubble separation
Author(s)	Maruyama, Hideo; Seki, Hideshi; Matsukawa, Yasuhiro et al.
Citation	Chemical Engineering Journal, 141(1-3), 112-118 https://doi.org/10.1016/j.cej.2007.11.001
Issue Date	2008-07-15
Doc URL	https://hdl.handle.net/2115/38773
Type	journal article
File Information	Maruyama_etal_08_authorversion.pdf



Hokkaido University Collection of Scholarly and Academic Papers : HUSCAP

Adsorption Behavior of Bisphenol-A and Diethyl Phthalate onto Bubble Surface in Nonfoaming Adsorptive Bubble Separation

Hideo Maruyama*, Hideshi Seki, Yasuhiro Matsukawa, Akira Suzuki, Norio Inoue

Laboratory of Bioresources Chemistry, Division of Marine Biosciences, Graduate School of Fisheries Science, Hokkaido University
Minato 3-1-1 Hakodate 041-8611, JAPAN
TEL:+81-138-408813; FAX:+81-138-408811; E–mail: maruyama@elsie.fish.hokudai.ac.jp

* Corresponding author
E–mail address: maruyama@elsie.fish.hokudai.ac.jp (H. Maruyama)

Abstract

To clarify adsorption equilibrium relationship at liquid-atmosphere interface, adsorption behavior of bisphenol-A (BPA) and diethyl phthalate (DEP) onto bubble surface was studied by using nonfoaming adsorptive bubble separation (NFBS) technique. The adsorption isotherm of BPA and DEP were obtained experimentally. The experimental results showed that adsorption equilibrium of BPA and DEP on bubble surface followed Langmuir's adsorption isotherm. Two adsorption parameters, the adsorption equilibrium constant and the saturated adsorption density on bubble surface could be determined and were 2.04×10^{5} cm^3/g and 1.35×10^{-8} g/cm^2 for BPA and 9.41×10^{4} cm^3/g and 1.79×10^{-8} g/cm^2 for DEP, respectively.

Keywords: nonfoaming adsorptive bubble separation, endocrine disruptor chemical, bisphenol-A, diethyl phthalate, separation

1. Introduction

Recently influences of environmental distributed chemicals, so called as endocrine disrupting chemicals (EDCs), on human, vertebrate and so on have been reported [1-8]. Among EDCs, bisphenol-A (BPA) is well known one and its influences of hormonal signals and irreversible effects on the development of the reproductive organs. Especially, many reports of these influences on fish have appeared in literature [9-15]. Fish and shellfish are important for human as not only protein resources but also resources of physiologically active and bioactive substances. For conservation and restoration of the aquatic environments, these substances is attempted to remove from aqueous environments. To this purpose, several techniques have been attempted and developed, i.e., adsorption method using solid adsorbent [16-20], degradation using ozone and ultraviolet light irradiation [21], degradation by catalyzed or enzymatic method [22, 23] and degradation by ultrasonic sound irradiation [24].

On the other hand, many EDCs have hydrophobic functional groups in their structure [25-27]. The authors focus on the hydrophobicity of EDCs and suppose that the adsorption phenomenon of EDCs at liquid-air interface will be utilized to remove EDCs from aqueous environments. Among them, nonfoaming adsorptive bubble separation (NFBS) [28, 29] and ultrasonic atomization techniques [30] have been proposed to remove/enrich surface-active substances from dilute aqueous solution [28-30]. Especially, ultrasonic atomization technique can be effective and potential method to remove EDCs due to its high ability of producing the specific surface area based on volume of liquid, i.e.,

liquid-atmosphere interfacial area [31]. For the process design of this method, adsorption behavior of EDCs at liquid-atmosphere interface should be important to determine adsorption equilibrium relationship. The NFBS technique is also available methods for not only a tool of investigation of adsorption behavior onto bubble surface of surface-active substances diluted in aqueous media but also removal of these substances in dilute solution, and has some advantages, i.e., low energy requirements, a little mechanical parts in the apparatus, no–requirement of tedious treatments such as desorption or addition of any other chemicals and extending to a continuous operation with ease.

In this study, nonfoaming adsorptive bubble separation (NFBS) experiments were conducted with bisphenol-A (BPA) and diethyl phthalate (DEP) as model EDCs, which have different value of partition coefficient n-octanol/water (log K_{ow}), respectively. The aim of this study is determination of adsorption equilibrium parameters of BPA and DEP. Determination of the adsorption parameters for EDCs is important to develop and design the further removal process.

2. Materials and Methods

2.1. Materials

Bisphenol-A (BPA) and diethyl phthalate (DEP) were purchased from Kanto Chemical Co. Inc. (Tokyo, Japan) and were used without further purification. These were dissolved in distilled water containing 1.0 wt.% NaCl. The solutions were used in experiments in this study. All experiments were conducted at room temperature and under atmospheric pressure.

2.2. Experimental Setup

A schematic diagram of the experimental setup for NFBS method is shown in Fig. 1. The setup is almost the same as that used in the previous study [28, 29, 32]. A bubble column consisting of a cylindrical acrylic resin tube of 4.4 cm I.D. and 36 cm in height was constructed. Sintered glass filter (10-15 μm mean-pore size) was installed as a gas distributor at the bottom of the column. Air was supplied to the column through the distributor. Pressure taps for measuring gas holdup in the column were installed at intervals of 25 cm along the wall.

The droplet trap and the droplet collector were used to measure the volumetric flow rate, q, and to determine the concentration, C_{tr}, of the droplet, respectively. They were equipped at the top of the column when they were used. The droplet trap was also made of an acrylic resin cylinder 1.8 cm in height and 5.0 cm in inside diameter (i.e., the outside diameter of the foam separation

column), the bottom end of the cylinder being covered with a stainless steel net. The trap was filled with a certain amount of cotton fiber wool and fixed at the top of the foam separation column.

During the experiment, the trap was filled with a certain amount of cotton to entrap droplets generated at the liquid–atmosphere interface. The detailed drawing of the collector is shown in Fig. 2. The droplet collector was made of transparent plastic resin and was consisted of a conical upper section with a cone angle of 75° and a cylindrical lower section with a diameter of 5.0 cm and a height of 3.2 cm. A suction tap of stainless steel pipe (0.3 μm in inside diameter) was attached to the top of the cone and it was connected to a reservoir for droplet recovery. To minimize droplet drying, four glass tubes were installed at the wall of the cylindrical part to induce humidified air.

2.3. Experimental Procedure

2.3.1. Measurement of droplet flow rate

An experimental setup used in this study is almost the same as that described in the previous paper [28, 29] as shown in Fig. 1. 500 mL of BPA or DEP solution was prepared at a desired concentration and it was charged into the column. Nitrogen gas or air was supplied to the column through a distributor. The droplet trap was made of acrylic cylinder with a steel mesh at the bottom end. At the experiment the trap was filled with a certain amount of cotton, and it was placed at the column top to entrap droplets generated at the

liquid-atmosphere interface.

Bisphenol-A (BPA) and diethyl phthalate (DEP) were used as model endocrine disruptors. The experiment for measuring volumetric flow rate of droplets was carried out as follows. BPA and DEP were dissolved in 1 wt.% NaCl solution, respectively, since, in some cases, environmental water has some ionic strength. A BPA or DEP solution prepared at a desired concentration was charged into the column up to a desired liquid level. Then, aeration was started and the trap was exposed to the upward flow of droplets generated at the liquid surface. After a certain time, the trap was detached from the column and it was weighed with a balance. The volumetric flow rate, q, of droplets was determined from the change in weight of the trap and the exposure time, assuming that the density of solution was equal to that of water. The experiments were repeated at various distance, H, which corresponds to the distance between the bottom of the droplet trap and the liquid surface within the column.

The intrinsic flow rate, q_0, of the droplets at the liquid surface within the column was determined by the extrapolation method [28, 29]; plots of q versus H yielded straight line with negative slope. The extrapolation of the line back to $H = 0$ gave q_0.

The gas holdup, ε_g, was determined from the difference in static pressure between the clear and aerated liquids using a differential pressure transducer (Tem-Tech Lab. Inc., JAPAN). The voltage signals from the transducer were recorded by a personal computer (NEC PC–9801VM) via A/D converter (CONTEC). All the experiments were conducted with a constant superficial gas velocity, $U_g = 5.37\times10^{-2}$ cm/s.

2.3.2. Enrichment experiment

The experimental setup and procedure were almost the same as those described in the previous paper [28, 29]. The experiments were operated in batchwise with respect to liquid. Each run was conducted for 30 minutes with U_g = 5.37×10^{-2} cm/s. As the preliminary experiments showed that C_{tr} was not changed with the position of the collector in the range of 1.4 - 4.4 cm, all the experiments were carried out at the constant position of 2.4 cm. The concentrations of BPA and DEP were measured spectrophotometrically at 285 nm for BPA, and 245 or 280 nm for DEP, respectively.

4. Results and Discussion

4.1. Determination of surface adsorption density of BPA and DEP

Taking into account that the objective surface-active substance contained in droplets is originated from the adsorbed at bubble-liquid interface and the dissolved in bulk liquid, the mass balance can be expressed as [28, 29, 32]:

$$q_0 C_{tr} = S_b X + q_0 C_b, \quad (1)$$

where, C_b, S_b and X denote concentration in the bulk liquid, the production rate of bubble surface area in the column and the surface density (amount of adsorbed on bubble surface in equilibrium), respectively. From Eq.(1) and Lagmuir's adsorption isotherm,

$$X = (q_0/S_b)(C_{tr} - C_b) = K\gamma C_b/(1 + KC_b), \quad (2)$$

where, K and γ represent the adsorption equilibrium constant and the saturated surface density (maximum amount of adsorbed on bubble surface in equilibrium), respectively. The production rate of bubble surface area in the column, S_b, is expressed by the following equation [28]:

$$S_b = 6A\varepsilon_g(1-\varepsilon_g)^{4.65}\{(4/225)(\rho_l-\rho_g)^2 g^2/(\mu_l\rho_l)\}^{1/3}, \quad (3)$$

where A, ε_g, g, ρ_l, ρ_g and μ_l denote a cross-sectional area of the column, the gas holdup, the gravitational acceleration, the densities of the liquid and the gas and the viscosity of the liquid, respectively.

4.2. Gas holdup and the intrinsic volumetric flow rate of droplet

Gas holdup, ε, and the intrinsic volumetric flow rate, q_0, of droplet at liquid-atmosphere interface within the column were determined. The results are shown in Figs. 3 and 4, respectively. The values of q_0 were determined by the extrapolation method [28, 29]. The axial profile of q for BPA is shown in Fig. 5 as a typical result. The gas holdup increased with C_i linearly in the present experimental range. On the other hand, the both profiles of q_0 have a bending points in the vicinity of ca. $C_i = 1.5\times10^{-5}$ M and ca. 2.0×10^{-5} M for BPA and DEP, respectively. The profile of ε is considered to reflect a statement of dispersed bubbles, i.e., bubble frequency and the average size of the dispersed bubbles in the solution within the column. The average diameter, d_b, of bubble swarm can be calculated by the following equation [32, 33]:

$$d_b = U_g / [\varepsilon_g(1-\varepsilon_g)^{4.65}\{(4/225)(\rho_l-\rho_g)^2 g^2/(\mu_l\rho_l)\}^{1/3}], \quad (4)$$

where, U_g represents a superficial gas velocity in the column. Fig. 6 shows the calculated values of d_b with function of the initial concentration, C_i, of the bulk liquid within the column. As seen in the figure, value of d_b decreased abruptly in the vicinity of ca. 1.0×10^{-5} M $< C_i <$ 2.0×10^{-5} M for both BPA and DEP. This

concentration range correspond to that of the bending points of q_0 for BPA and DEP. Up to the bending point, increase in q_0 seemed to be affected by rather increase in the bubble frequency. At higher concentration over the bending point, unstable foam was generated and was accumulated at the edge between the inside column wall and the liquid surface within the column. This is unstable foam collapsed immediately when the aeration was stopped. As increased the initial concentration of the bulk liquid, this unstable foam intends to decrease the effective cross-sectional area at liquid/air interface where droplet generated. Thus, the degree of increasing q_0 decreased over the bending point.

4.3. Adsorption isotherm of BPA and DEP

Figs. 7a and 7b show the adsorption isotherms for BPA and DEP. To reveal the difference of the amounts adsorbed for BPA and DEP in the lower concentration region (ca. $C_i < 3.0\times10^{-6}$ M), the ordinate and the abscissa of Fig. 5b are expressed in logarithmic scale. The ordinate of Figs. 7a and 7b represent the adsorption density, X, of EDCs on bubble surface, which correspond to $(q_0/S_b)(C_{tr}–C_b)$ in Eq. (2). In this calculation, the initial concentration of the bulk liquid, C_i, was regarded as the bulk concentration, because the volume of the initial solution is much larger than that of the collected mist droplets. Thus, the authors employed C_i as C_b hereafter. This tendency was observed in our previous study dealing with crystal violet and humic acid [29].

On the other hand, a reciprocal of Eq. (2) is written as:

$$\frac{S_b}{q_0(C_{tr}-C_i)}=\frac{1}{K\gamma}\cdot\frac{1}{C_i}+\frac{1}{\gamma}. \quad (5)$$

Eq. (5) shows the Langmuir plot in the present adsorption system. The slope and the intercept of the straight line give the values of K and γ, respectively.

Fig. 8 shows the plot of Eq. (5) for BPA and DEP, respectively. Straight lines in Fig. 8 were calculated by a least-squares method. As seen in Fig. 8, the both data for BPA and DEP are in good agreement with Eq. (5). This fact supports that the adsorption equilibrium relationship of BPA and DEP onto bubble surface should follow the Langmuir adsorption isotherm. From the intercept and the slope of each line, the values of adsorption equilibrium constant, K, and the saturated surface density, γ, for BPA and DEP were determined. These values are summarized in Table 1.

4.4. Adsorption parameters

Interpretation of physical meanings of adsorption equilibrium constant, K, is so complicated. In the present system, however, K seems to reflect the hydrophobicity of surface active substances. The partition coefficient *n*-octanol/water is well known as an index parameter of hydrophobicity (log K_{ow}). Thus, K_{ow} should indicate a degree of hydrophobicity of objective substance. The values for both BPA and DEP were reported; 2.47 for DEP [34], and, 3.32 [35], 3.82 [36], 3.84 [37], 3.40 [38], and 3.43 [39] for BPA. The value for BPA is larger than that for DEP, although the reported values for BPA have

some scatter. This tendency is similar with the case of K determined in this study. The logarithm value of ratio of partition coefficient *n*-octanol/water of BPA and DEP is ranged in 1.34 - 1.55, on the other hands, the ratio of K for BPA and DEP is 2.16. The value of the ratio of K is rather larger than that of the partition coefficient *n*-octanol/water.

4.5. Verification of Enrichment Ratio

For verification of the adsorption parameters, K and γ, determined in the present study, the experimental E values were compared with the calculated ones. From Eqs. (1) and (2), the enrichment ratio, E, can be expressed as:

$$E \equiv C_{tr}/C_i = 1 + (S_b/q_0)\, K\gamma / (1+KC_i) \tag{7}$$

From Fig. 4, q_0 is apparently affected by the initial concentration, C_i, of solution. Thus, the value of q_0 can be approximated by linear regression (solid lines in Fig. 4).

In case of BPA,

for $C_i \leq 1.0\times10^{-5}$ M

$$q_0 = 3.44\times10^{2}\, C_i + 2.38\times10^{-3} \tag{8}$$

for $1.0\times10^{-5} < C_i \leq 3.0\times10^{-4}$ M

$$q_0 = 1.39\times10^{1}\, C_i + 6.05\times10^{-3} \tag{9}$$

In case of DEP,

for $C_i \leq 1.0\times10^{-5}$ M

$$q_0 = 3.90\times10^{2}\, C_i + 2.22\times10^{-3} \quad (10)$$

for $1.0\times10^{-5} < C_i \leq 2.5\times10^{-4}$ M

$$q_0 = 1.08\times10^{1}\, C_i + 6.16\times10^{-3} \quad (11)$$

The value of gas holdup, ε, can be also estimated experimentally by linear regression (solid lines in Fig. 3).

In case of BPA,

$$\varepsilon = 2.33\times10^{1}\, C_i + 5.20\times10^{-3} \quad (12)$$

In case of DEP,

$$\varepsilon = 1.52\times10^{1}\, C_i + 5.20\times10^{-3} \quad (13)$$

The value of intercept of Eqs. (12) and (13), 5.20×10^{-3}, corresponds to the value of gas holdup of 1.0 wt.% NaCl solution. By means of the relations of Eqs. (8) - (13), Eqs. (2) and (3), and the adsorption parameters (K and γ), the E value can be calculated semi-theoretically. Fig. 9 shows comparison of the experimental E values and the calculated ones for BPA and DEP. Data in this figure is different from Figs. 7 and 8 and was obtained by other series of enrichment experiments for BPA and DEP, respectively for verification of the parameters and the reproducibility of the present experiments. The experimental range of C_i were $1.0\times10^{-6} \leq C_i \leq 1.0\times10^{-4}$ M for DEP and $1.0\times10^{-6} \leq C_i \leq 3.0\times10^{-4}$ M for BPA,

respectively. As for BPA, slightly higher C_i region could be employed in the enrichment experiments for the verification, in comparison with the C_i range in estimation of the adsorption parameter (Figs 7 and 8). The good agreement between the experimental E and the calculated E can be recognized in Fig. 9. This suggests that the present method is reproducible and that the estimated adsorption parameters should be valid.

Conclusion

Nonfoaming adsorptive bubble separation (NFBS) experiments were conducted with bisphenol-A (BPA) and diethyl phthalate (DEP) as the model endocrine disruptor chemicals (EDCs). The adsorption isotherms for BPA and DEP were obtained and agreed well with Langmuir's plot of the present system. Thus, the adsorption equilibrium relationship between bulk liquid and bubble surface for both BPA and DEP was expressed by Langmuir's adsorption isotherm. According to Langmiur's plot, two adsorption parameters, the adsorption equilibrium constant, K, and the saturated adsorption density, γ, on bubble surface could be determined and were 2.04×10^{5} cm^3/g and 1.35×10^{-8} g/cm^2 for BPA and 9.41×10^{4} cm^3/g and 1.79×10^{-8} g/cm^2 for DEP, respectively.

Notation

A	a cross-sectional area of bubble column	$[m^2]$
C_b	concentration of bulk liquid	$[kg/m^3]$
C_i	initial concentration of bulk liquid	$[kg/m^3]$
C_{tr}	concentration of liquid droplets	$[kg/m^3]$
d_b	average diameter of bubble swarm dispersed within the column defined by Eq. (4)	[m]
g	the gravitational acceleration	$[m/s^2]$
H	distance between the bottom of the droplet trap and the liquid surface within the column	[m]
K	adsorption equilibrium constant	$[m^3/kg]$
L	Avogadro's number	[-]
M_w	molecular weight	[kg/mol]
q	volumetric flow rate of liquid droplets	$[m^3/s]$
q_0	intrinsic volumetric flow rate of liquid droplets	$[m^3/s]$
S_b	production rate of bubble surface area	$[m^2]$
U_g	superficial gas velocity	[m/s]
X	adsorption density on bubble surface	$[kg/m^2]$

Greek symbols

ε_g	gas holdup	[-]
γ	saturated surface adsorption density on bubble surface	$[kg/m^2]$

ρ_g	gas density	$[kg/m^3]$
ρ_l	liquid density	$[kg/m^3]$
μ_l	liquid viscosity	[kg/(m s)]

References

[1] B. Jimènez, Trends Anal. Chem. 16 (1997) 596-606.

[2] F.R. Knudsen, T.G. Pottinger, Aquat. Toxicol. 44 (1999) 159-170.

[3] I. Lutz, W. Kloas, Sci. Total Environ. 225 (1999) 49-57.

[4] W. Kloas, I. Lutz, R. Einspanier, Sci. Total Environ. 225 (1999) 59-68.

[5] J.J.A. Mendes, Food Chem. Toxicol. 40 (2002) 781-788.

[6] T.B. Hayes, Integr. Comp. Biol. 45 (2005) 321-329.

[7] F. Grün, H. Watanabe, Z. Zamanian, L. Maeda, K. Arima, R. Cubacha, D.M. Gardiner, J. Kanno, T. Iguchi, B. Blumberg, Mol. Endocrinol. 20 (2006) 2141-2155.

[8]C. Porte, G. Janer, L.C. Lorusso, M. Ortiz-Zarragoitia, M.P. Cajaraville, M.C. Fossi, L. Canesi, Comp. Biochem. Physiol. C 143 (2006) 303-315.

[9] P. Sohoni , C.R. Tyler, K. Hurd, J. Caunter, M. Hetheridge, T. Williams, C. Woods, M. Evans, R. Toy, M. Gargas, J.P. Sumpter, Environ. Sci. Technol. 35 (2001) 2917-2925.

[10] A. Belfroid, M. Velzen, B. Horst, D. Vethaak, Chemosphere 49 (2002) 97-103.

[11] S. Kashiwada, H. Ishikawa, N. Miyamoto, Y. Ohnishi, Y. Magara, Water Res. 36 (2002) 2161–2166.

[12] H.J. Baek, M.H. Park, Y.D. Lee, H.B. Kim, Fish Physiol. Biochem. 28 (2003) 413-414.

[13] F. Lahnsteiner, B. Berger, M. Kletzl, T. Weismann, Aquat. Toxicol. 75 (2005) 213–224.

[14] M. Nagae, K. Shiroyama, M. Inoue, A. Hara, Y. Takao, S. Kohra, Y. Ishibashi, N. Tominaga, S. Yoshihara, K. Arizono, J. Health Sci. 51 (2005) 93-95.

[15] J.P. Sumpter, A.C. Johnson, Environ. Sci. Technol. 39 (2005) 4321-4332.

[16] A. Nakanishi, M. Tamai, N. Kawasaki, T. Nakamura, S. Tanada, J. Colloid Interface Sci. 252 (2002) 393-396.

[17] T. Emmerik, M.J. Angove, B.B. Johnson, J.D. Wells, M.B. Fernandes, J. Colloid Interface Sci. 266 (2003) 33-39.

[18] T. Kubo, K. Hosoya, T. Sano, M. Nomachi, N. Tanaka, K. Kaya, Anal. Chim. Acta 549 (2005) 45-50.

[19] H. Tsue, T. Takimoto, C. Kikuchi, H. Yanase, H. Takahashi, K. Amezawa, K. Ishibashi, S. Tanaka, R. Tamura, Chem. Lett. 34 (2005) 1030-1031.

[20] A. Shareef, M.J. Angove, J.D. Wells, B.B. Johnson, J. Colloid Interface Sci. doi:10.1016/j.jcis.2005.10.039.

[21] S. Irmak, O. Erbatur, A. Akgerman, J. Hazard. Mater. B126 (2005) 54-62.

[22] H.M. Coleman, K. Chiang, R. Amal, Chem. Eng. J. 113 (2005) 65-72.

[23] K. Modaressi, K.E. Taylor, J.K. Bewtra, N. Biswas, Water Res. 39 (2005) 4309-4316.

[24] N.B. Abderrazik, A. Azmani, C. R'kiek, W. Song, K.E. O'Shea, Catal. Today 101 (2005) 369-373.

[25] R. Liu, A. Wilding, A. Hibberd, J.L. Zhou, Environ. Sci. Technol. 39 (2005) 2753-2761.

[26] J.H. Kwon, H.M. Liljestrand, L.E. Katz, Environ. Toxicol. Chem. 25 (2006) 1984-1992.

[27] H. Yamamoto, H.M . Liljestrand, Y. Shimizu, M. Morita, Environ. Sci. Technol. 37 (2007) 2646-2657.

[28] A. Suzuki, H. Maruyama, H. Seki, T. Hayashi, J. Chem. Eng. Jpn. 28 (1995) 115-117.

[29] A. Suzuki, H. Maruyama, H. Seki, J. Chem. Eng. Jpn. 29 (1996) 794-798.

[30] A. Suzuki, H. Maruyama, H. Seki, Y. Matsukawa, N. Inoue, Ind. Eng. Chem. Res. 45 (2006) 830-833.

[31] Y. Matsukawa, H. Maruyama, H. Seki, A. Suzuki, Proceedings of the 15th annual meeting of Hokkaido branch, society of chemical engineers, Japan (2006) 47-50. (in Japanese)

[32] A. Suzuki, H. Maruyama, J. Colloid Interface Sci. 238 (2001) 54-61.

[33] H. Maruyama, A. Suzuki, H. Seki, N. Inoue, Biochem. Eng. J. 30 (2006) 253-259.

[34] Material safety data sheet, Kanto Chemical, Co. Inc. (2006) No. 14189.

[35] Y.I. Korenman, A.A. Gorohkov, Zhurnal Prokladnoi Khimii. 46 (1973) 2597-2599.

[36] F.A. Blanchard, Log Kow and BCF for BPA. Dow Chemical Company technical memorandum submitted to the U.S. Environmental Protection Agency, Washington, DC. 1984.

[37] P.B. Dorn, C. Chou, J.J. Gentempo, Chemosphere 16 (1987) 1501-1507.

[38] B. Leverkusen, Grunddatensatz fuer Altsoffe ueber 1000 JATO. 1989.

[39] J. Hu, T. Aizawa, Water Res. 37 (2003) 1213-1222.

List of figure captions and table titles

Fig. 1. Schematic diagram of experimental setup for nonfoaming adsorptive bubble separation.

Fig. 2. detail drawing of droplet collector for determining the concentration, Ctr, of droplet in nonfoaming adsorptive bubble separation experiment.

Fig. 3. Change in gas holdup, ε, with the initial bulk concentration, C_i, within the column for bisphenol-A (BPA; open circle) and diethyl phthalate (DEP; open triangle). Solid lines were calculated by a least squares regression.

Fig. 4. Change in the intrinsic volumetric flow rate, q_0, of liquid droplet at liquid-atmosphere interface within the column as a function of the initial bulk concentration, C_i, of the bulk liquid for bisphenol-A (BPA; open circle) and diethyl phthalate (DEP; open triangle). Solid lines are calculated by a least squares regression.

Fig. 5. Axial profiles of the volumetric flow rate, q, of droplets at air-liquid interface within the column with the initial concentration, C_i, for bisphenol-A(BPA) in nonfoaming adsorptive bubble separation.

Fig. 6. Variation of the average diameter, d_b, of bubbles dispersed within the column with the initial bulk concentration, C_i for bisphenol-A (BPA; opencircle)

and diethyl phthalate (DEP; open triangle). The plotted data were calculated from Eq. (4).

Fig. 7. The adsorption isotherms of bisphenol-A (BPA; open circle) and diethyl phthalate (DEP; open triangle) onto bubble surface.

Fig. 8. Fitting of the data of Fig. 5 to Eq. (5) for bisphenol-A (BPA; open circle) and diethyl phthalate (DEP; open triangle).

Fig. 9. Comparison of the values of experimental enrichment ratio, *E* and the calculated ones for bisphenol-A (BPA; open circle) and diethyl phthalate (DEP; open triangle).

Table 1. Adsorption parameters determined in the present study.

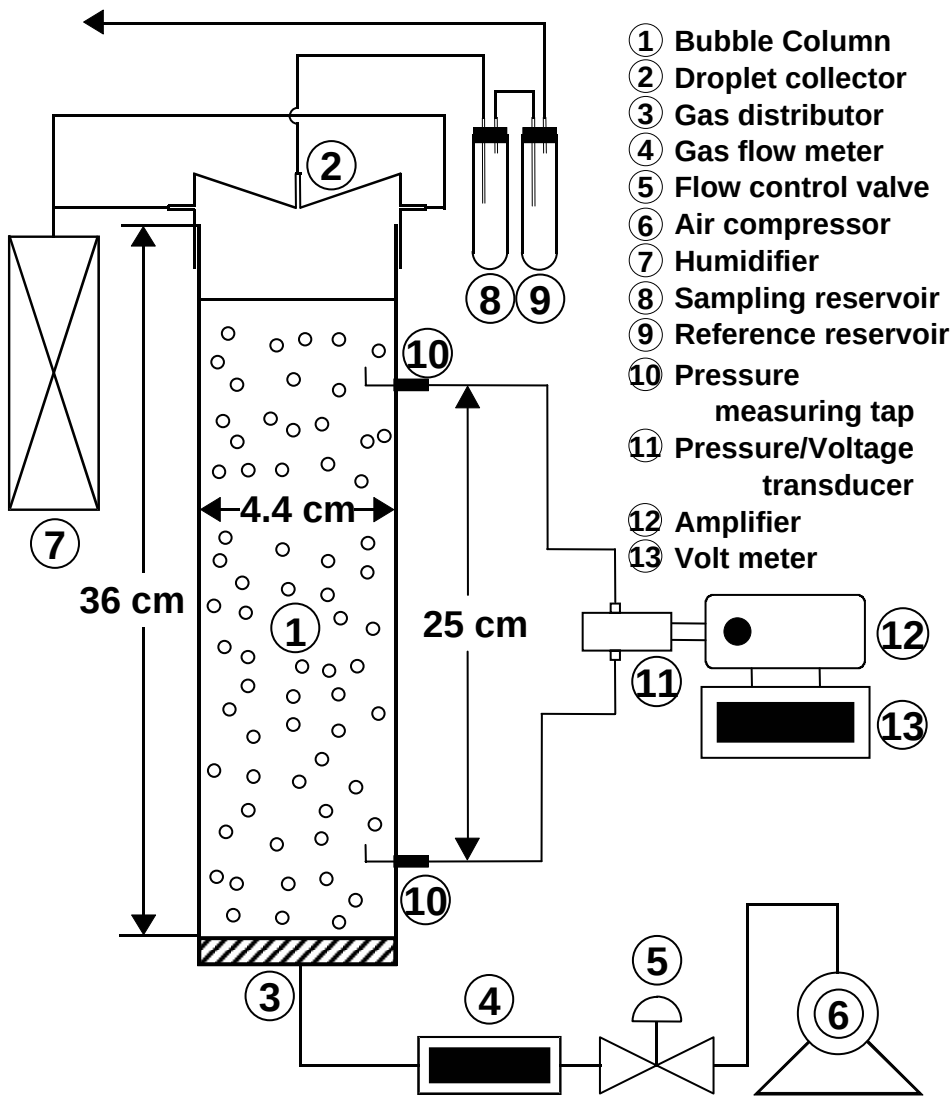


Fig. 1. Schematic diagram of experimental setup for nonfoaming adsorptive bubble separation.

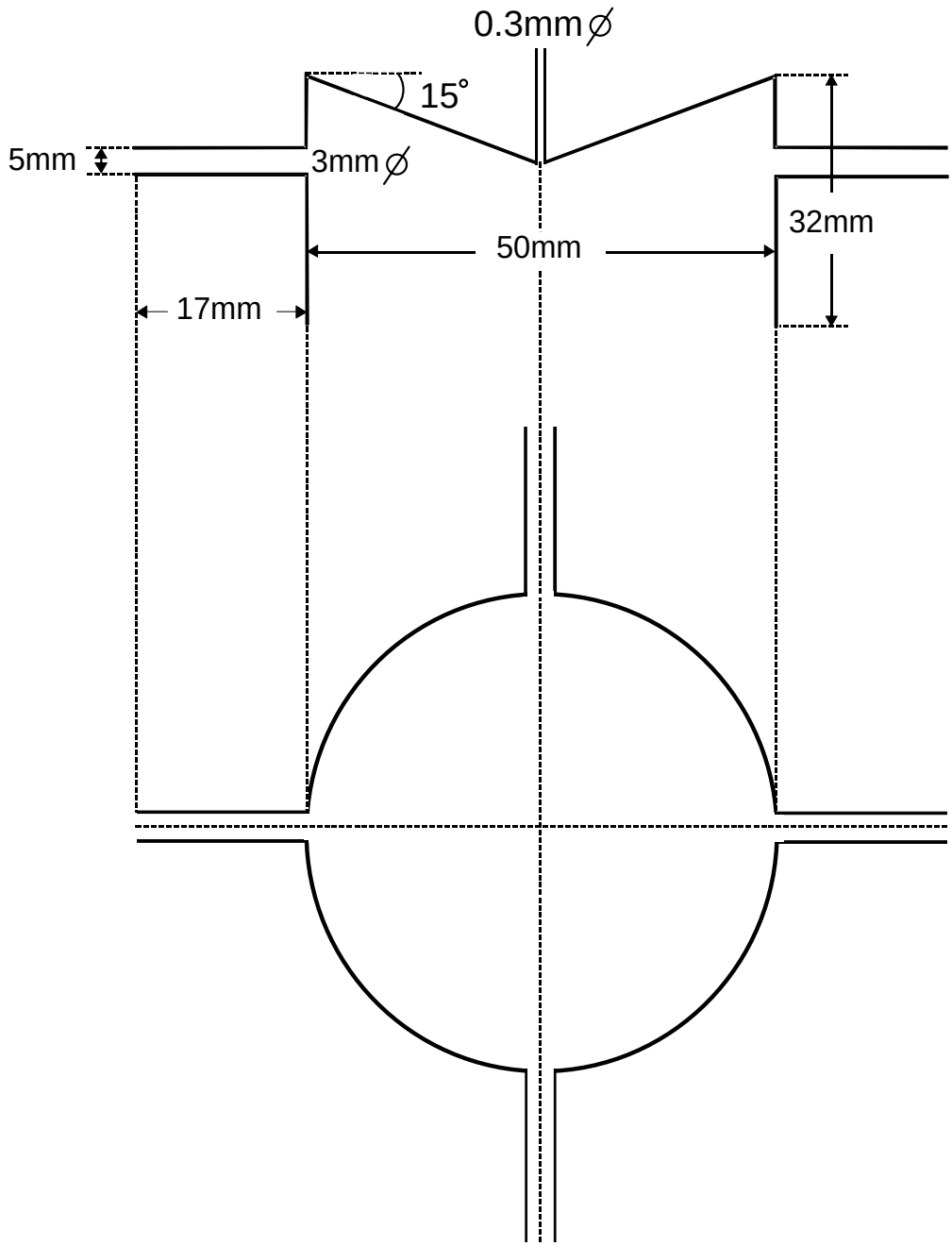


Fig. 2. detail drawing of droplet collector for determining the concentration, C_{tr}, of droplet in nonfoaming adsorptive bubble separation experiment.

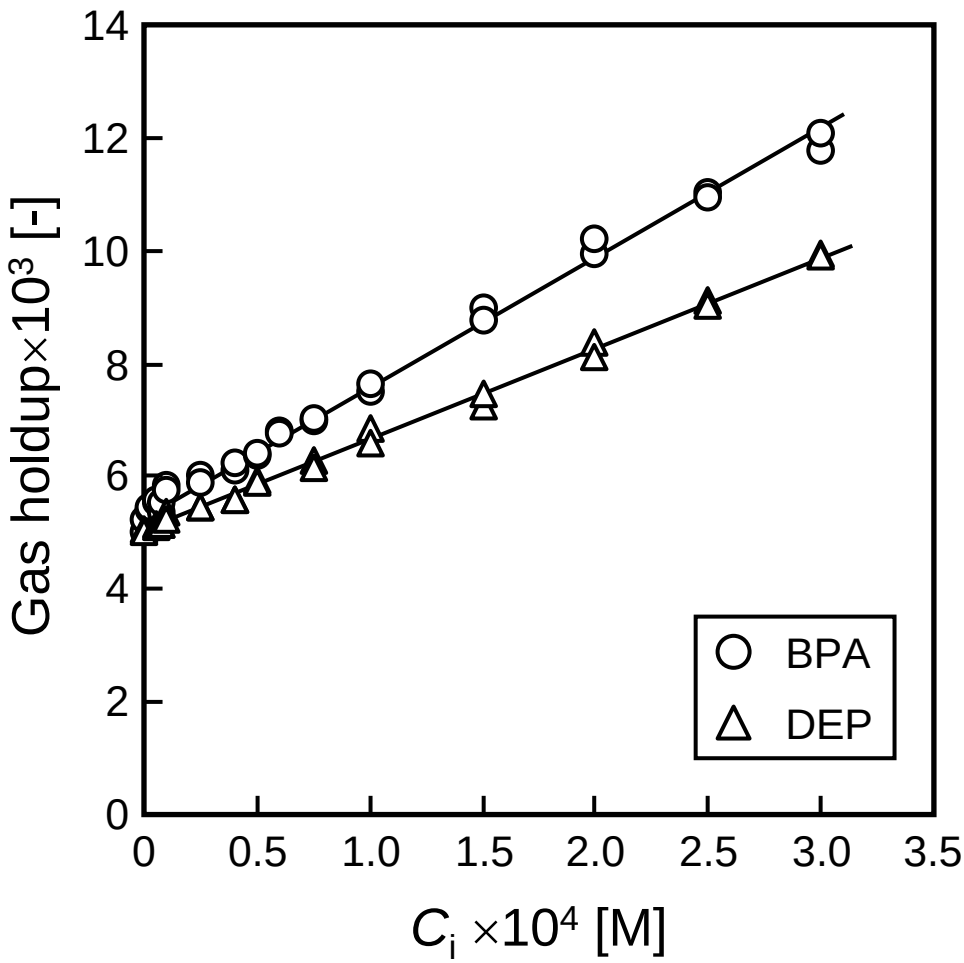


Fig. 3. Change in gas holdup, ε, with the initial bulk concentration, C_i, within the column for bisphenol-A (BPA; open circle) and diethyl phthalate (DEP; open triangle). Solid lines were calculated by a least squares regression.

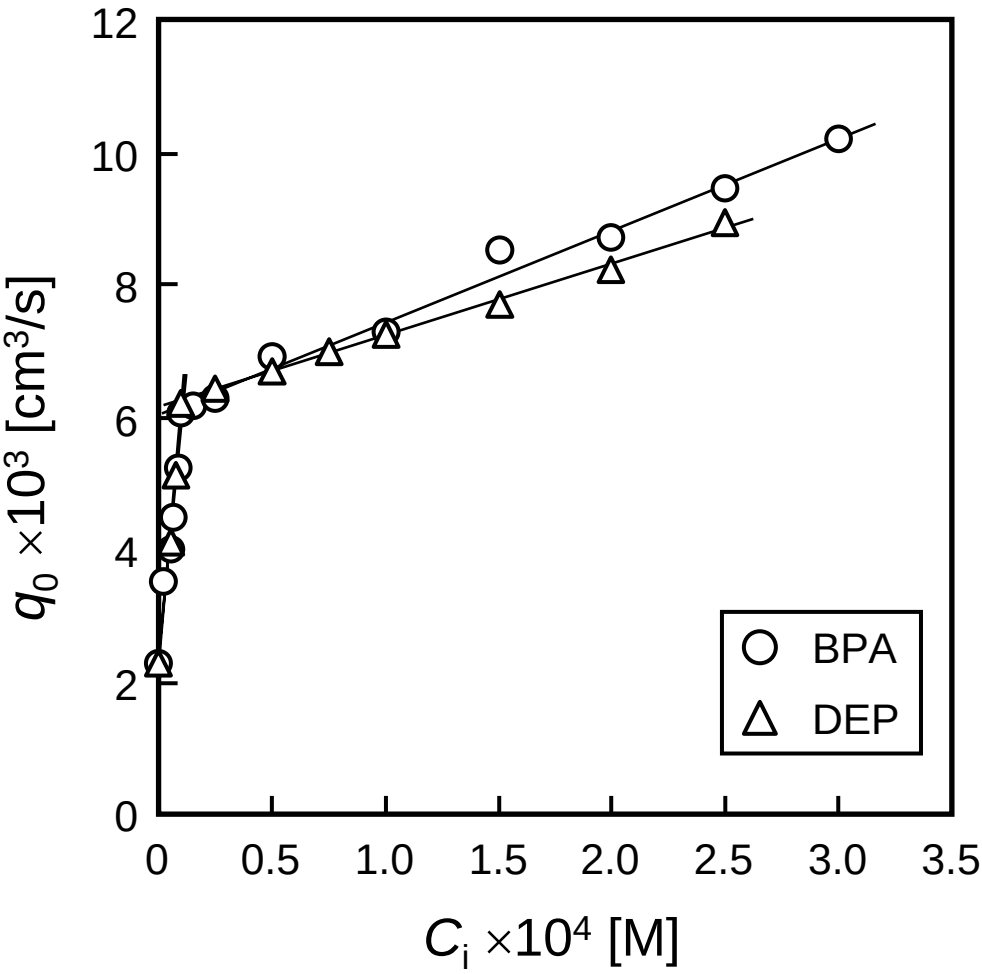


Fig. 4. Change in the intrinsic volumetric flow rate, q_0, of liquid droplet at liquid-atmosphere interface within the column as a function of the initial bulk concentration, C_i, of the bulk liquid for bisphenol-A (BPA; open circle) and diethyl phthalate (DEP; open triangle). Solid lines are calculated by a least squares regression.

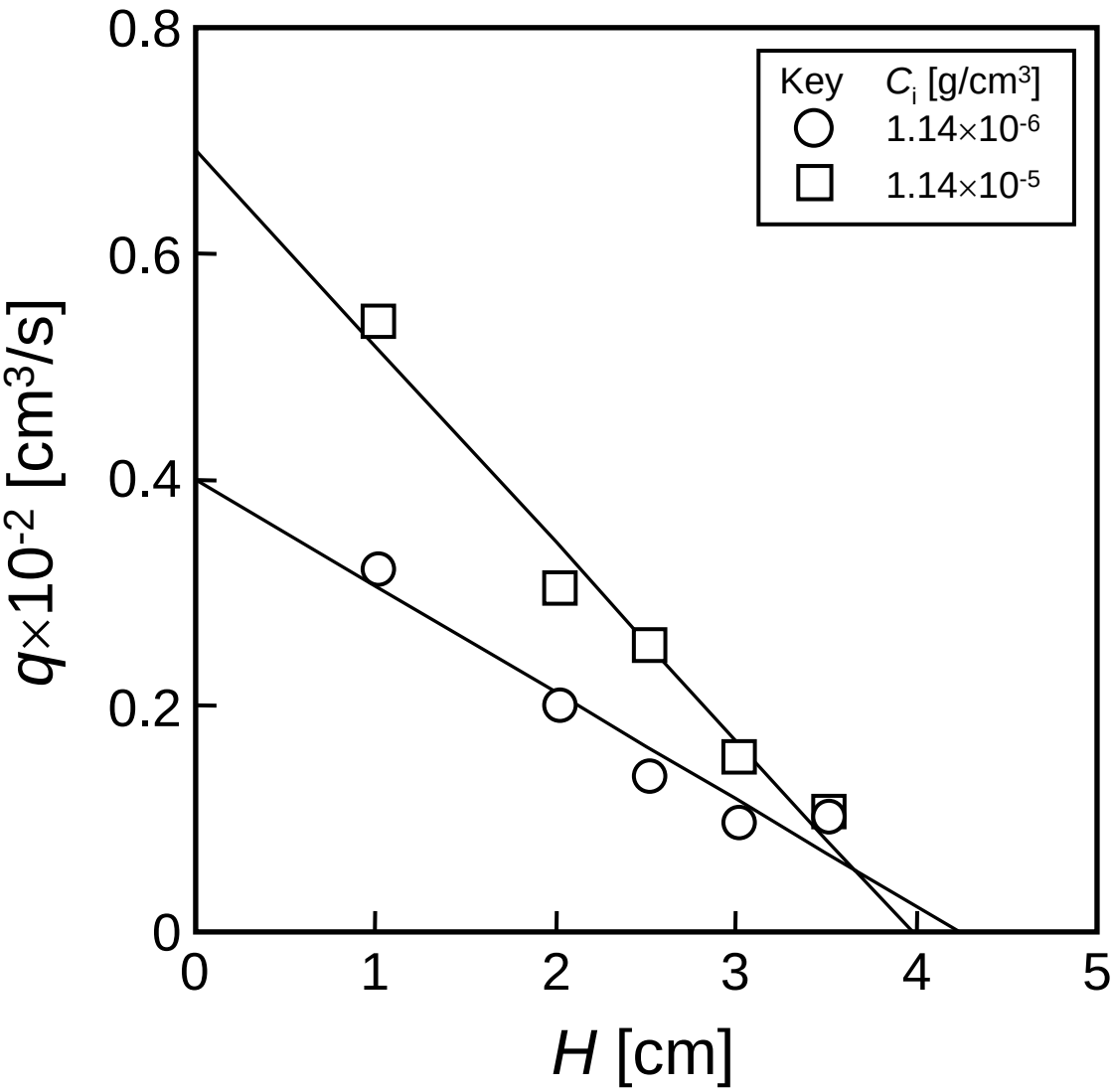


Fig. 5. Axial profiles of the volumetric flow rate, q, of droplets at air-liquid interface within the column with the initial concentration, C_i, for bisphenol-A(BPA) in nonfoaming adsorptive bubble separation.

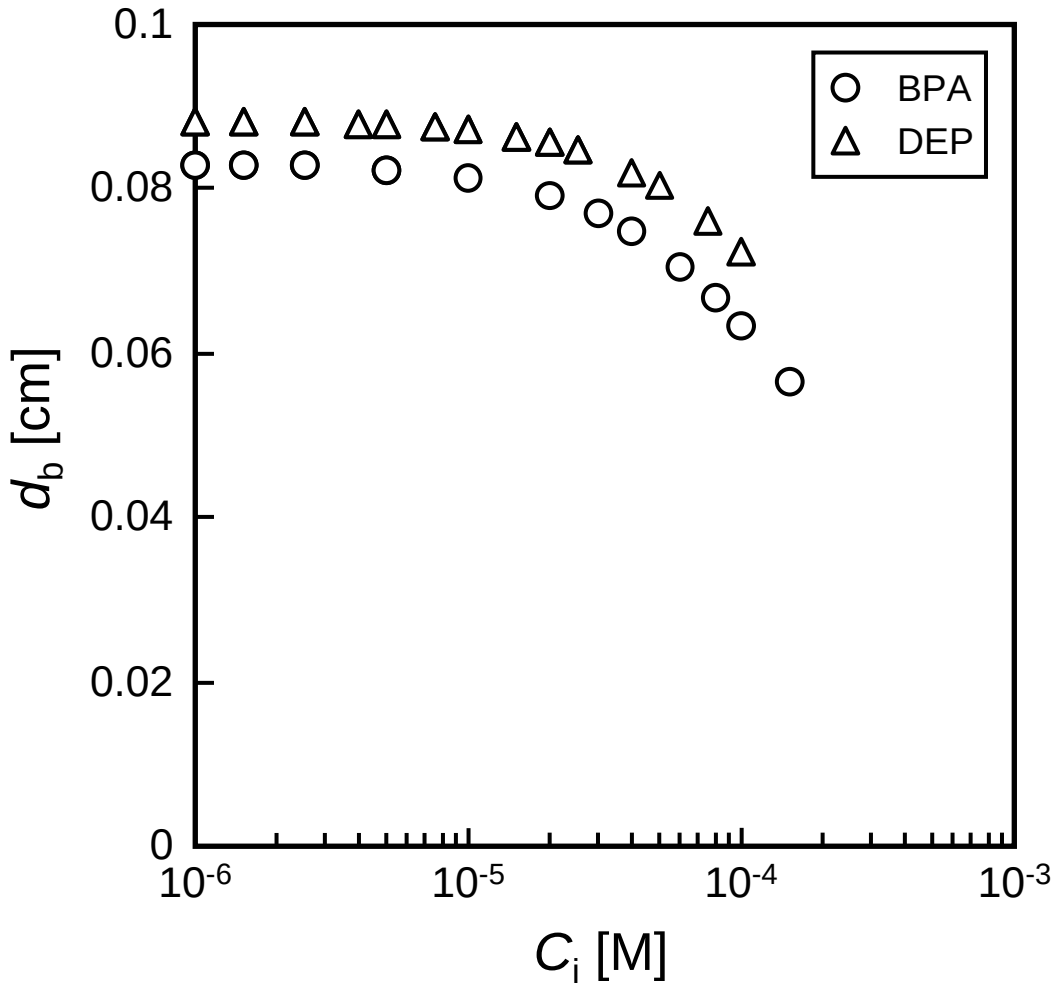


Fig. 6. Variation of the average diameter, d_b, of bubbles dispersed within the column with the initial bulk concentration, C_i for bisphenol-A (BPA; opencircle) and diethyl phthalate (DEP; open triangle). The plotted data were calculated from Eq. (4).

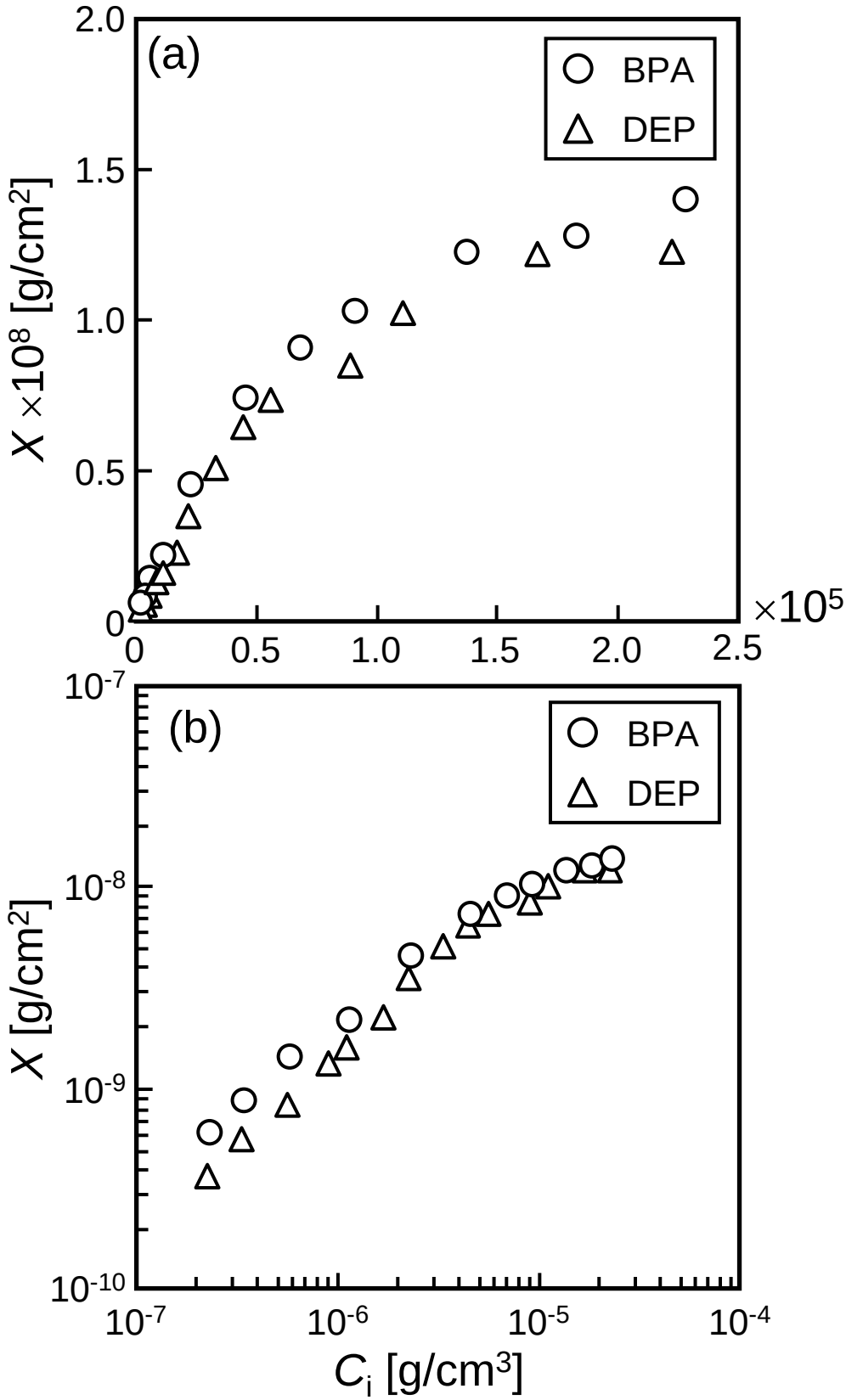


Fig. 7. The adsorption isotherms of bisphenol-A (BPA; open circle) and diethyl phthalate (DEP; open triangle) onto bubble surface.

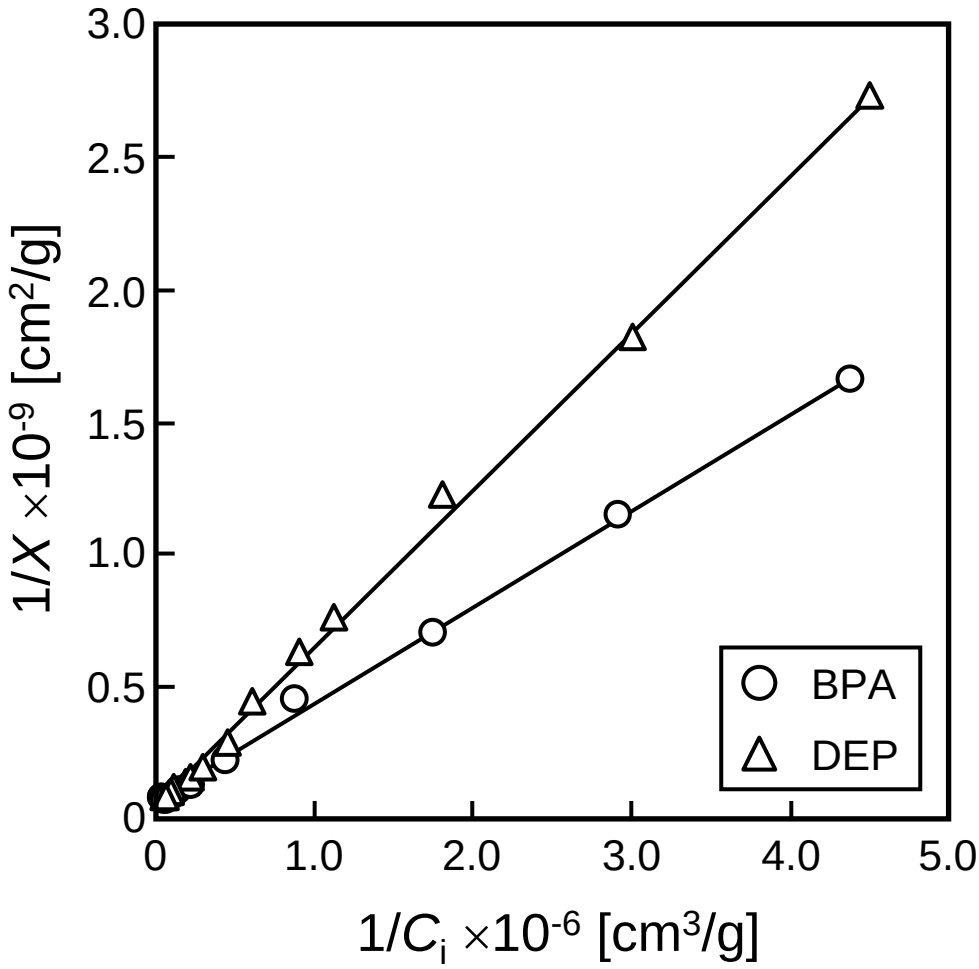


Fig. 8. Fitting of the data of Fig. 5 to Eq. (5) for bisphenol-A (BPA; open circle) and diethyl phthalate (DEP; open triangle).

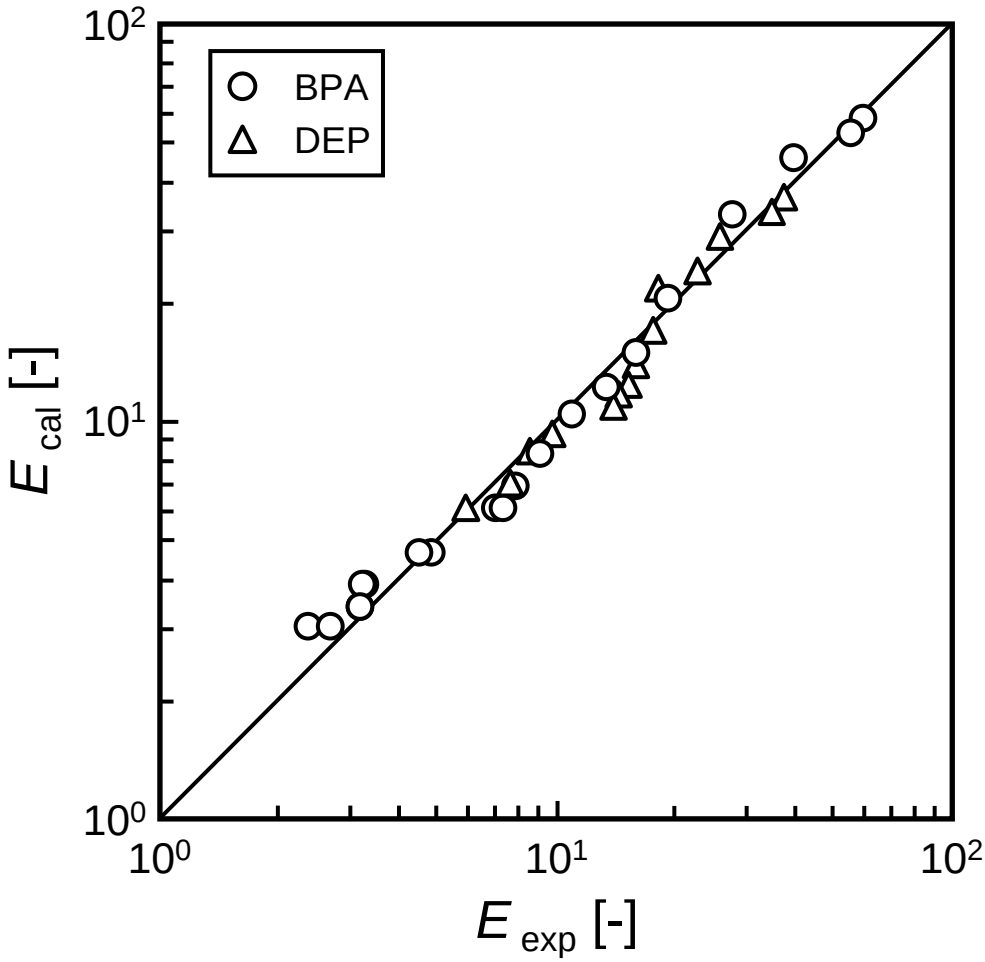


Fig. 9. Comparison of the values of experimental enrichment ratio, *E* and the calculated ones for bisphenol-A (BPA; open circle) and diethyl phthalate (DEP; open triangle).

Table 1. Adsorption parameters determined in the present study

	K [cm^3/g]	γ [g/cm^2]
BPA	2.04×10^{5}	1.35×10^{-8}
DEP	9.41×10^{4}	1.79×10^{-8}